Journal of Medicinal Chemistry

ARTICLE

pubs.acs.org/jmc

Polyalkoxybenzenes from Plants. 5. Parsley Seed Extract in Synthesis of Azapodophyllotoxins Featuring Strong Tubulin Destabilizing Activity in the Sea Urchin Embryo and Cell Culture Assays

Marina N. Semenova,[†,‡] Alex S. Kiselyov,[§] Dmitry V. Tsyganov,[∥] Leonid D. Konyushkin,[∥] Sergei I. Firgang,[∥] Roman V. Semenov,[∥] Oleg R. Malyshev,[∥] Mikhail M. Raihstat,[∥] Fabian Fuchs,[⊥] Anne Stielow,[⊥] Margareta Lantow,[⊥,#] Alex A. Philchenkov,[▽] Michael P. Zavelevich,[▽] Nikolay S. Zefirov,[○] Sergei A. Kuznetsov,[⊥] and Victor V. Semenov*[,†,∥]

[†]Institute of Developmental Biology, RAS, 26 Vavilov Street, 119334 Moscow, Russian Federation

[‡]Chemical Block Ltd., 3 Kyriacou Matsi, 3723 Limassol, Cyprus

[§]CHDI Foundation, 6080 Center Drive, Suite 100, Los Angeles California 90045, United States

[∥]N. D. Zelinsky Institute of Organic Chemistry, RAS, 47 Leninsky Prospect, 119991 Moscow, Russian Federation

[⊥]Institute of Biological Sciences, University of Rostock, 3 Albert-Einstein-Strasse, D-18059 Rostock, Germany

[#]Department of Pathology, Immunology and Laboratory Medicine, University of Florida, 1600 Archer Road, Gainesville Florida 32610, United States

[▽]R. E. Kavetsky Institute of Experimental Oncology, Pathology, and Radiobiology, National Academy of Sciences of Ukraine, 45 Vasyl′kivska Street, 03022 Kyiv, Ukraine

[○]Lomonosov Moscow State University, GSP-1, Leninskie Gory, 119991 Moscow, Russian Federation

Supporting Information

ABSTRACT: A series of 4-azapodophyllotoxin derivatives with modified rings B and E have been synthesized using allylpolyalkoxybenzenes from parsley seed oil. The targeted molecules were evaluated in vivo in a phenotypic sea urchin embryo assay for antimitotic and tubulin destabilizing activity. The most active compounds identified by the in vivo sea urchin embryo assay featured myristicin-derived ring E (**4e**, **6e**, and **8e**). These molecules were determined to be more potent than podophyllotoxin. Cytotoxic effects of selected molecules were further confirmed and evaluated by conventional assays with A549 and Jurkat human leukemic T-cell lines including cell growth inhibition, cell cycle arrest, cellular microtubule disruption, and induction of apoptosis. The ring B modification yielded 6-OMe substituted molecule **8e** as the most active compound. Finally, in Jurkat cells, compound **8e** induced caspase-dependent apoptosis mediated by the apical caspases-2 and -9 and not caspase-8, implying the involvement of the intrinsic caspase-9-dependent apoptotic pathway.

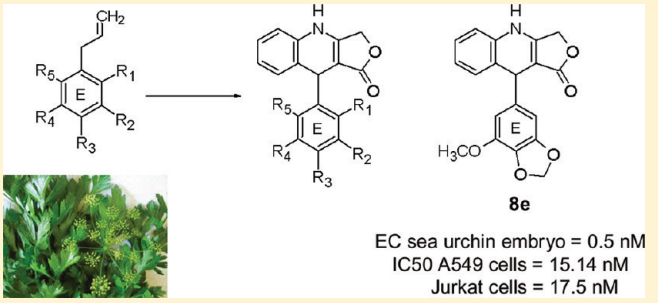

INTRODUCTION

Podophyllotoxin (PT) (Figure 1) is a lignan of aryltetralin family found in plants of *Podophyllum* genus. It is a strong microtubule destabilizing agent that binds to the colchicine site of tubulin.[1,2] PT and its derivatives exhibit anticancer, antiviral, and insecticide activities based on their ability to dissociate microtubules.[3−9] However, clinical trials of PT as an anticancer agent were unsuccessful due to its considerable toxicity.[3] Numerous attempts have been made to improve PT safety profile while maintaining its potency. For example, semisynthetic PT derivatives, including etoposide (Figure 1), teniposide, and etopophos, are currently in clinical use for the treatment of a variety of malignancies. A reported mechanism of action for these compounds is distinct from that of the parent PT and involves strong DNA-topoisomerase II inhibition leading to late S-G2 cell cycle arrest and subsequent apopotosis.[10−13] An alternative nontubulin and nonantitopoisomerase mode of action for some PT derivatives has been proposed recently, associated with cell death and sub-G1 apoptotic cell accumulation without any significant cell cycle arrest.[11,14]

PT structure (Figure 1) features four chiral centers, making it a challenge for the structure−activity relationship studies. Absolute stereochemistry of substituents at the C_1 atom (the ring C) was reported to have major influence on compound's antitumor activity.[3] Several synthetically feasible structural analogues of PT

Received: June 8, 2011
Published: September 15, 2011

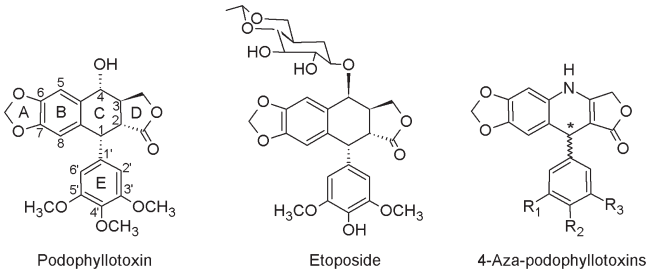

Figure 1. Structures of podophyllotoxin, etoposide, and general structure of synthesized 4-aza-analogues.

were designed to address epimerization at positions 1−4.[3] For example, 4-aza-PT derivatives with a chiral center C_1 (Figure 1) showed antiproliferative and pro-apoptotic activity in HeLa and Jurkat cells (**4a** and **18a**)[15,16] and inhibited growth of human liver cancer cells $HepG_2$ (**4a** and **4i**).[17] Two racemic analogues of 4-aza-PTs (**4a** and **6a**) were more cytotoxic against P388 murine leukemia cells than the parent PT.[18,19] Several 4-aza-PT derivatives were reported to be potent tumor inhibitors (ex., **4a**)[20] and vascular-disrupting agents.[21] In addition, insecticidal (larvicidal) activity possibly mediated by microtubule alterations was reported for this class of molecules.[6] However, experimental evidence for the mechanism of action and cellular targets of 4-aza-PTs has been obtained only recently. Namely, it was shown that some of 4-aza-PTs with hetero aryl, benzo hetero aryl, or tetrahydronaphthalene rings A and B exhibited cytotoxicity involving microtubule depolymerization, G2/M cell cycle arrest, and apoptotic cell death.[22,23]

Considering synthetic feasibility, antimitotic, antiproliferative, and tubulin destabilizing activity of 4-aza-PT derivatives, these compounds continue to attract a considerable interest. In the present study, we prepared a series of 4-aza-PT derivatives using plant polyalkoxybenzenes easily available from parsley and dill seed extracts.[24,25] It has been suggested that rotation of the axial E-ring in the parent PT molecule is restricted as it is almost orthogonal to the other rings.[26] Therefore a modification of the rings B and E with additional methoxy functionality could affect the rotation of the ring E yielding PT derivatives with promising antimitotic potencies. Moreover, tetraalkoxybenzene pharmacophore is featured in several natural products with reported antiproliferative activity including *Cactaceae* tetrahydroisoquinolines[27] and flavonoids and isoflavonoids.[28−30]

In designing the evaluation sequence for test molecules, we aimed at identifying potent novel aza-analogues of PT and confirming their specific antitubulin activity via a variety of cell-based assays. The initial in vivo sea urchin embryo assay allowed for the identification of hits featuring desirable antimitotic potency and phenotypic effect (vide infra) in comparison with the parent molecule (PT). This primary screen based on the simple organism model has been carried out to yield active molecules that were likely to affect tubulin dynamics as shown by us earlier.[31−34] Tubulin targeting activity of these compounds would be further confirmed in A549 human lung epithelial carcinoma cell line. A detailed insight into the effects of selected active compounds on cellular proliferation, cell cycle progression, and microtubule distribution in cultured A549 cells was intended to confirm their specific tubulin destabilizing mode of action. Moreover, the link between compound-induced microtubule disruption and respective downstream intracellular mechanisms responsible for initiation of caspase-mediated apoptotic events was studied.

Scheme 1[a]

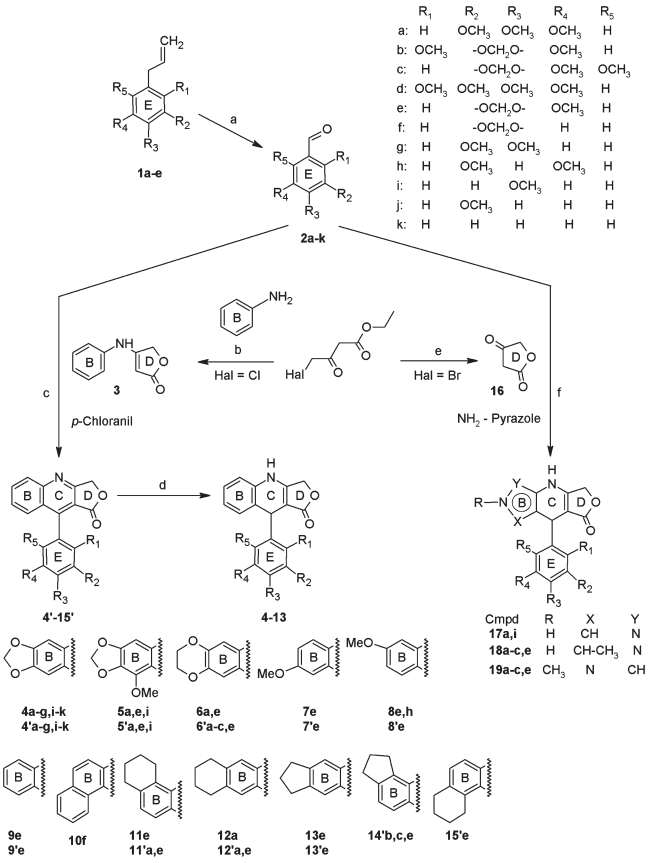

	R_1	R_2	R_3	R_4	R_5
a:	H	OCH_3	OCH_3	OCH_3	H
b:	OCH_3	$-OCH_2O-$		OCH_3	H
c:	H	$-OCH_2O-$		OCH_3	OCH_3
d:	OCH_3	OCH_3	OCH_3	OCH_3	H
e:	H	$-OCH_2O-$		OCH_3	H
f:	H	$-OCH_2O-$		H	H
g:	H	OCH_3	OCH_3	H	H
h:	H	OCH_3	H	OCH_3	H
i:	H	H	OCH_3	H	H
j:	H	OCH_3	H	H	H
k:	H	H	H	H	H

Cmpd	R	X	Y
17a,i	H	CH	N
18a-c,e	H	$CH-CH_3$	N
19a-c,e	CH_3	N	CH

[a] Reagents and conditions: (a) (i) powdered KOH, $(n\text{-Bu})_4N^+Br^-$, heat, 100 °C, 40 min; (ii) O_3, $CHCl_3$−MeOH−pyridine (80:20:3 v/v), −15 °C, 1−2 h;[25] (b) C_6H_6−AcOH, reflux, 8 h; (c) CF_3COOH, rt, 24 h; (d) AcOH−$NaBH_3CN$, rt, 15 h; (e) ref 43; (f) EtOH−Et_3N, reflux, 3 h. Compounds **4**−**13** (**f**−**k**), **17i**, **18e**, **19e** were synthesized from the corresponding commercial aldehydes.

All molecules were evaluated in a phenotypic sea urchin embryo assay in order to assess their antiproliferative and tubulin-destabilizing activities.[31] The assay includes (i) fertilized egg test for antimitotic activity displayed by cleavage alteration/arrest and (ii) behavioral monitoring of a free-swimming blastulae treated immediately after hatching. In our earlier validation efforts, we concluded that lack of forward movement, settlement to the bottom of the culture vessel and rapid spinning of an embryo around the animal−vegetal axis suggests a tubulin-destabilizing activity caused by a molecule (video illustrations are available at http://www.chemblock.com). An assay setup provides the possibility to identify a molecule with antimitotic or nonspecific cytotoxic activity and a novel mode of action.[32] Data generated by the sea urchin embryo assay have been further confirmed using conventional cell-based and in vitro tubulin polymerization assays.[33,34] As a result, we identified several promising candidates for the advanced in vivo evaluation.

CHEMISTRY

4-Aza-PTs **4**−**13** and intermediate quinolines **4′**−**15′** were synthesized as described earlier[6,15−20,35−37] via the cyclization of 4-chloro-acetoacetic acid with the corresponding amines, followed by the addition of aldehydes **2a**−**k** in the presence of an

Table 1. Effects of 4-Aza-podophyllotoxins on Sea Urchin Embryo and Cancer Cells

	sea urchin embryo effects EC (nM)[a]			cytotoxicity IC_{50} (nM)		
compd	cleavage alteration	cleavage arrest	embryo spinning	A549[b]	P388[c]	A549 cell total microtubule disruption (μM)[d]
PT	20	50	500	7.47 ± 0.41	10.4	0.1
etoposide	2000	>68000	>68000	7140[e]	1180[e]	ND[f]
4a	50	500	2000	2.71 ± 0.92	4.5	0.1
4′a	>4000	>4000	>4000	11928.33 ± 5368.30	>252900	>5
4b	1000	2000	>5000	ND[f]	ND[f]	ND[f]
4c	100	500	4000	ND[f]	ND[f]	ND[f]
4d	1000	4000	>10000	299.32 ± 58.35	ND[f]	1
4e	5	50	50	55.18 ± 7.54	ND[f]	1
4f	10	50	200	ND[f]	85.4	ND[f]
4g	5	100	2000	595.58 ± 46.18	130.7	1
4i	50	200	2000	>3200	385.4	ND[f]
4j	5	20	100	ND[f]	15.7	ND[f]
4k	5	20	100	63.00 ± 5.21	17.2	ND[f]
5a	2000	>2000	>2000	291.43 ± 143.53	ND[f]	5
5e	50	500	2000	297.63 ± 164.54	ND[f]	>5
5i	2000	>2000	>2000	ND[f]	ND[f]	ND[f]
6a	200	1000	1000	9.20 ± 1.22	4.1	1
6e	5	50	100	64.67 ± 11.34	ND[f]	0.5
7e	10	50	500	282.27 ± 96.99	ND[f]	5
8e	0.5	5	50	15.14 ± 2.98	ND[f]	1
8h	2	10	200	ND[f]	ND[f]	ND[f]
9e	20	200	2000	533.83 ± 111.47	ND[f]	>5
10f	>4000	>4000	>4000	ND[f]	ND[f]	ND[f]
11e	5	50	100	159.05 ± 8.24	ND[f]	ND[f]
11′e	200	2000	5000	ND[f]	ND[f]	ND[f]
12a	50	200	100	56.54 ± 6.83	ND[f]	0.5
13e	2	20	50	264.09 ± 52.32	ND[f]	5
13′e	100	1000	>5000	ND[f]	ND[f]	ND[f]
14′e	100	>4000	>5000	ND[f]	ND[f]	ND[f]

[a] The sea urchin embryo assay was conducted as described previously;[31] fertilized eggs and hatched blastulae were exposed to 2-fold decreasing concentrations of compounds; duplicate measurements showed no differences in effective threshold concentration (EC) values. [b] A549: human lung epithelial carcinoma cells; data are expressed as the mean ± SD from the dose−response curves of three independent experiments. [c] P388: murine leukemia cells; data from ref 19. [d] A549 cells were incubated with compounds at concentrations of 0.1, 0.5, 1, and 5 μM during 8 h. Data are expressed as compound concentration that caused total microtubule disassembly from three independent experiments (see Figure 4B,D−F as an example). [e] Data from ref 44. [f] ND: not determined.

oxidizing reagent *p*-chloranil (Scheme 1). Aldehydes **2a**−**e** were synthesized using natural polyalkoxybenzenes extracted from parsley seed oil.[25] For the SAR study, a panel of 4-aza-PTs with the ring E derived from commercially available aldehydes **2f**−**k** has been obtained. Quinolines **4′**−**13′** were reduced with $NaBH_3CN$ in a glacial acetic acid to yield compounds **4**−**13** in 12−86% yields. 4-Aza-PTs **4**−**13** were stable as solids, however, they were readily oxidized to respective quinolines **4′**−**13′** when dissolved in DMSO or ethanol. Dihydropyridopyrazole derivatives **17**−**19** were obtained by a three-component condensation of respective aminopyrazole, aldehyde **2**, and tetronic acid **16** as reported in the literature.[16] Notably, compounds **4g**, **4′g**, **4f**, and **4′f** are aza-analogues of the natural lignans taiwanin C and chinensin.[36,38−42]

RESULTS AND DISCUSSION

All synthesized aza-PTs **4**−**19** and **4′**−**15′** were evaluated for their antiproliferative, antimitotic, and microtubule destabilizing activities using in vivo sea urchin embryo assay. Cytotoxicity, cellular microtubule depolymerization, and apoptosis-inducing effects of selected compounds have been further assessed using A549 human lung epithelial carcinoma and Jurkat human leukemic T-cell lines.

Evaluation of 4-aza-PTs in the Phenotypic Sea Urchin Embryo Assay. Effects of 4-aza-PTs on the sea urchin embryo are summarized in Table 1 and Table S1 of the Supporting Information. PT and etoposide were used as references.

As evidenced from Table 1, a number of 4-aza-PTs (**4a**,**c**,**e**−**g**, **i**−**k**, **5e**, **6a**,**e**, **7e**, **8e**,**h**, **9e**, **11e**, **11′e**, **12a**, and **13e**) displayed significant cleavage alteration, cleavage arrest, and embryo spinning, suggesting their antimitotic microtubule destabilizing activity. Figure 2 illustrates typical developmental changes of an embryo when treated with a representative compound **4e**. The observed phenotypic changes suggest direct tubulin dynamic effects of 4-aza-PT derivatives. Interestingly, molecules **4a**, **4e**, and **8h** were reported as larvicidal agents against *Phaedon cochleariae* beetle, whereas **4j**, **4k**,

dx.doi.org/10.1021/jm200737s |*J. Med. Chem.* 2011, 54, 7138–7149

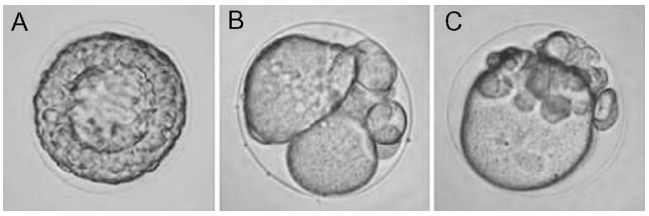

Figure 2. Effect of **4e** on sea urchin embryo development. Time after fertilization (21 °C): 6 h. (A) Intact embryo at early blastula stage. Fertilized eggs were exposed continuously to **4e** at 10 nM (B) and 100 nM (C). Note abnormal cleavage of cells with different size and shape that are irregularly positioned and formation of large multinucleated blastomeres (B). Tuberculate shape of an arrested egg seen on (C) is typical for tubulin destabilizing agents.

and **8h** were toxic against *Spodoptera frugiperda* larvae.[6] We believe that less potent compounds **4b**,**d**, **18e**, **6′b**, and **13′e** were tubulin destabilizers as well, although they did not cause embryo spinning. As evidenced from the detailed microscopic analysis, these compounds induced formation of tuberculate eggs typical of tubulin destabilizers (Figure 2C).[31] In our hands, topoisomerase inhibitor etoposide featured cleavage alteration but failed to induce cleavage arrest and embryo spinning. When applied to hatched blastulae, etoposide at 4−5 μM caused larval (pluteus) malformations. At higher concentrations (10−20 μM), marked abnormalities of gastrulation and morphogenesis were detected, whereas at 40−68 μM, developmental abnormalities and eventual embryo death were observed after 2.5 h of treatment.

Because of their marginal solubility in DMSO, ethanol, and seawater, we were unable to test **8′e**, **11′a**, and **12′a** or reach higher concentrations for **4b**,**d**, **18e**, **6′b**, and **13′e**. **14′e** showed nontubulin antiproliferative activity, as evidenced by the lack of embryo spinning and arrested tuberculate eggs.

Structure−Activity Studies in the Sea Urchin Embryo Assay. *1. The Ring C: Saturated vs Unsaturated Compounds.* A number of 1,4-aza-PT analogues (**4a**−**g**,**i**−**k**, **5e**, **6a**,**e**, **7e**, **9e**, and **13e**) featuring 1,4-dihydropyridine system for the ring C exhibited potent antimitotic activity with EC_{50} values of 0.5 nM−2 μM in the sea urchin assay. These results are in agreement with the published data.[19] Conversely, the respective aromatic pyridine derivatives **4′a**−**g**,**i**−**k**, **5′e**, **6′a**,**e**, **7′e**, **9′e**, and **13′e**) were inactive up to 4 μM concentration or exhibited moderate cleavage alteration effect (Table 1; Table S1, Supporting Information), with a notable exception of **11′e**, featuring myristicin substituent for the ring E. This molecule did exhibit a tubulin destabilizing activity although it was significantly lower than that for the corresponding unsaturated analogue **11e**. In addition, aromatization of the ring C yielded decrease in cytotoxicity and microtubule effects, presumably due to the inactive conformation of the ring E.[3]

Several saturated compounds were found to lose their activity in DMSO solution at room temperature. For example, the antimitotic effect of **4k** on sea urchin embryos decreased significantly (by ca. 5-fold) within 2 days after storage in DMSO. According to the literature data, aromatization of **4a** to yield **4′a** required harsh experimental conditions such as refluxing acetic acid.[37] We observed this conversion to take place in DMSO at room temperature, as confirmed by the time course NMR studies of **4k**. Specifically, in 2 and 6 days, the rate of its conversion to the respective aromatic analogue **4′k** were 25% and 45%, respectively. A similar activity reduction was observed for **4i** and **6a**,

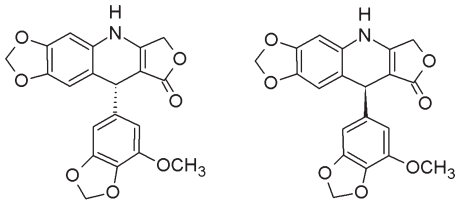

R-isomer *S*-isomer

Figure 3. Structures of **4e** enantiomers.

whereas DMSO stocks of compounds **4f**, **8e**, **9e**, and **11e** retained their activities for 2−4 days.

2. Other Substitutions: Rings A, B, and E. Introduction of a methoxy-group to C_8 position of the ring B dramatically decreased antiproliferative activity in sea urchin embryo assay (Table 1, compounds **4a** ≫ **5a**, **4e** ≫ **5e**, and **4i** ≫ **5i**). Replacement of methylenedioxy group (the ring A) with ethylenedioxy substituent did not result in a definitive outcome. For example, the potency of respective ethylenedioxy derivative (Table 1, **4a** vs **6a**) in the sea urchin embryo cleavage stages was reduced significantly, similar to the reported insecticidal activity.[6] However, for the pair **4e** vs **6e**, the activity was not affected.[19] Replacement of the ring A with two methoxy substituents was reported to either result in a marked reduction of cytotoxicity[19,45,46] or was negligible.[16] Similar derivatives featuring a single methoxy group at C_7 displayed reduced potency compared to the parent 4-aza-PT molecule (Table 1, **4e** vs **7e**). On the contrary, 6-methoxy derivative **8e** exhibited the strongest antiproliferative effect of all tested 4-aza-PTs being ca. 40 times more potent than the parent PT. Another 6-methoxy analogue **8h** displayed high activity in the sea urchin assay as well as pronounced larvicidal effect.[6] Compound **9e** lacking the ring A was less active, however it did retain the antimitotic activity. Substitution of the ring A with cyclopentane moiety was reported to result in a moderate decrease in cytotoxicity.[19] In our assay system, this modification slightly enhanced the in vivo effect (Table 1, **4e** and **13e**), however a nontubulin antiproliferative activity of 5,6-cyclopentyl derivative **14′e** was also detected. In contrast, replacement of the ring A with a cyclohexyl group did not influence the antimitotic potency at the sea urchin embryo cleavage stages (Table 1, **4e** and **11e**; **4a** and **12a**). At later developmental stages of the embryo (ex., after hatching), **12a** displayed formidable toxicity. Similarly, cyclohexyl derivative **12a** exhibited cytotoxicity against human cervical (HeLa) and breast (MCF-7) carcinomas cells at nanomolar concentration range.[23]

A replacement of the AB ring system of 4-aza-PTs with pyrazole was reported to furnish derivatives that retained both cytotoxic and proapoptotic activities at 5 μM concentration.[15,16] However, cellular target(s) or mode of action for these molecules have not been determined. In our hands, all tested pyrazole-containing compounds **17a**,**i**, **18a**−**c**, and **19a**−**c**,**e** failed to affect sea urchin embryo development at any stage up to 4 μM concentration, the only exception being myristicin-derived **18e** that exhibited weak tubulin-destabilizing properties (Table S1, Supporting Information).

As described above, 1,4-dihydropyridine derivatives (the ring C) showed the best activities in the sea urchin embryo assay. We further evaluated the effect of C_1 substituent (the ring E) on compounds activity. Notably, molecules featuring *m*-methoxybenzene- or myristicin-derived substituent (Table 1, **4e**,**j**, **5e**, **6e**, **7e**, **8e**, **9e**, **11e**, and **13e**) consistently exhibited the highest potency. 2,3-Dimethoxy and

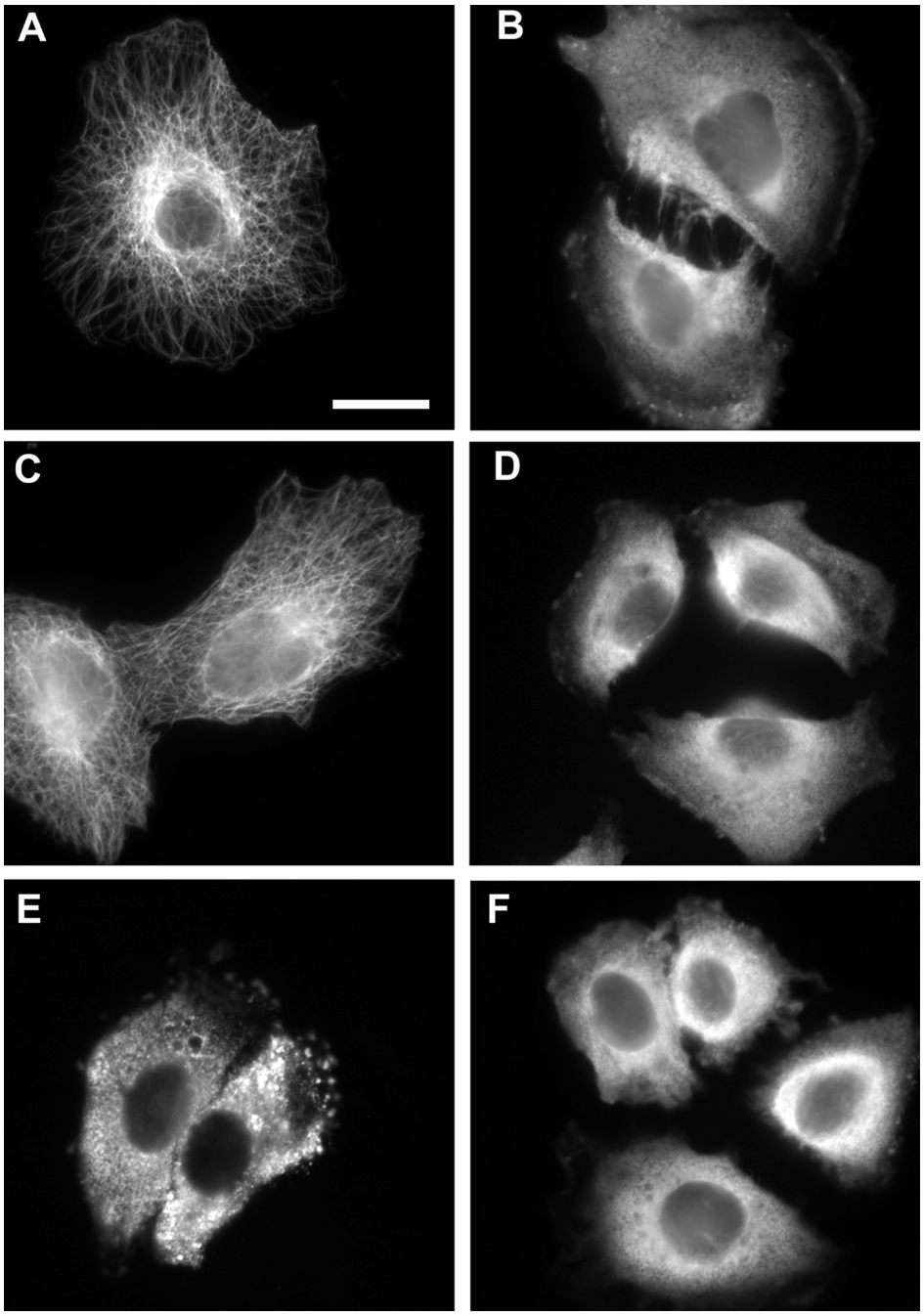

Figure 4. Effects of selected compounds on the interphase microtubule networks in A549 lung carcinoma cells as analyzed by indirect immunofluorescence microscopy. Cells were treated with 0.1% DMSO (A) and with test compounds (1 μM) for 8 h: **4a** (B), **4′a** (C), **4e** (D), **6a** (E), and **8e** (F). Bar: 25 μm. Note microtubule disappearance in B, D−F.

ethylenedioxy derivatives (ex., **4f,g**) were less potent, displaying activities slightly higher than the parent PT. (see Table 1). Respective *p*-methoxybenzene and 3,4,5-trimethoxybenzene analogues showed further reduced antitubulin effects in the assay (Table 1, **4a,i**, **5a,i**, and **6a**), whereas 4-aza-PT molecules substituted with dillapiol-, apiol-derived or tetramethoxybenzene moieties **4b**−**d** were the least active. Compound **4k** with unsubstituted benzene ring E exhibited strong antimitotic tubulin destabilizing activity, suggesting that methoxy groups in the ring E may not directly affect antitubulin activity. Similarly, 3′,4′,5′-demethoxy PT retained significant cytotoxicity.[47] For the molecules featuring 8-methoxy moiety, the myristicin-derived analogue **5e** displayed the highest activity (**5e** vs **5a,i**). A similar pattern was observed for the respective ethylenedioxy derivatives **6a** and **6e**.

In the next round of structure−activity studies, the effect of stereochemistry on compound's activity has been studied. It was reported previously that (+)-configuration of antitubulin isoquinoline derivatives was essential for their cytotoxicity and inhibition of tubulin polymerization.[48] For 4-aza-PTs, only *R*-enantiomer of **8h** was found to be cytotoxic against cultured insect cells and larvae, showing cellular behavior consistent with its microtubule effect.[6]

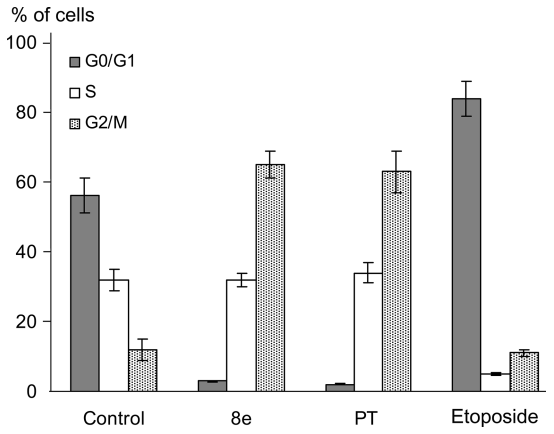

Figure 5. Cell cycle distribution of Jurkat cells treated with **8e** (20 nM), PT (25 nM), and etoposide (2 μM) for 24 h. The cells were stained with propidium iodide to analyze DNA content by flow cytometry.

Similarly, *R*-enantiomer of 4-aza-PT mimetic with naphthalene A,B-ring system was about 1000 times more potent in HeLa and MCF-7 cells than *S*-enantiomer.[23] In the present study, a racemic **4e** was separated by chiral HPLC to yield pure enantiomers (Figure 3 and Figure S1, Supporting Information). Both *R*-isomer and a respective racemate of **4e** were found to cause cleavage alteration and arrest of the sea urchin embryo at 5 and 50 nM, respectively. The respective *S*-isomer was less active, exhibiting cleavage abnormalities at 50 nM and cleavage arrest at 200 nM. Both enantiomers triggered embryo spinning, suggesting their tubulin destabilizing properties.

In summary, the sea urchin embryo profiling of the new aza-PT derivatives suggested that the most potent representative in each structural group featured myristicin-derived ring E (ex., **4e**, **5e**, **6e**, **8e**, **11e**, and **13e**, Table 1). Notably, methylenedioxy ring A was not required for the activity. For example, introduction of 6-methoxy or 7-methoxy groups into the ring B yielded potent molecules (ex., **7e**, **8e**, and **8h**).

Cell Growth Inhibitory Activity. Following outcome of the sea urchin embryo assay, we evaluated the inhibitory effect of selected active compounds on proliferation of A549 human lung carcinoma cells and Jurkat leukemia T-cells using MTT[49] and trypan blue assays, respectively. Relevant A549 cellular IC_{50} data for **4a**,**d**,**e**,**g**,**i**,**k**, **5a**,**e**, **6a**,**e**, **7e**, **8e**, **9e**, **11e**, **12a**, **13e**, **4′a**, and reference compounds (PT, etoposide) are summarized in Table 1. Reported cytotoxicity data for selected molecules against P388 murine leukemia cells are included as well (Table 1).[19] Notably, in Jurkat cells, **8e** and PT exhibited IC_{50} values of 17.5 and 25 nM, respectively.

In general, sensitivity of sea urchin embryos to 4-aza-PTs at the cleavage stage, when cells divide synchronously every 35−40 min, was markedly higher than that of cancer cells, probably due to their higher frequency of mitosis. Key features of the most active molecules identified in both assays included: (i) 1,4-dihydropyridine template for the ring C (**4a** vs **4′a**), (ii) a myristicin-derived substitution in the ring E (**8e**), (iii) 6-methoxy substituent replacing the ring A (**4e** vs **8e**), and (iv) lack of 8-methoxy substitution in the ring B (**4a** vs **5a**, **4e** vs **5e**). Results of structure−activity relationship studies for the ring E correlated well between both cellular (A549 and P388) and sea urchin embryo assays. Compounds **4f** and **4j** exhibited high cytotoxicity against P388 cells (Table 1).[19] Molecules featuring 3,4,5-trimethoxybenzene substituent (**4a** and **6a**) as well as the parent PT were the most cytotoxic agents against both human A549 and murine P388 cancer cell lines, **4a** being more potent than PT. Notably, derivatives endowed with the myristicin moiety showed the greatest antimitotic activities in sea urchin embryo assay. Similarly, in Jurkat cells a myristicin derivative **8e** was more potent than PT. Replacement of the ring A with cyclopentyl or cyclohexyl moieties markedly decreased cytotoxicity against A549 cells (**4e** vs **13e**; **4a** vs **12a**), but this effect was almost negligible in the sea urchin embryo test. The observed discrepancy could be attributed to the differences between mitotic spindle microtubules in frequently dividing sea urchin blastomeres vs predominantly interphase microtubules in cultured cancer cells targeted by tubulin destabilizing agents.

The Effect on Microtubule Distribution in Cells. Next, we evaluated the effect of selected active compounds on microtubule stability and distribution in cultured A549 cells. Specifically, cells were incubated with test articles (0.1−5 μM) or PT (0.1 and 5 μM) as a positive control and 0.5% DMSO as a negative control. Microtubules were subsequently labeled by the indirect immunofluorescence method and analyzed by fluorescence microscopy. Figure 4 exemplifies the microtubule destabilization effect of selected 4-aza-PTs in A549 cells.

As shown in Table 1, compounds **4a**,**d**,**e**,**g**, **6a**, **6e**, **7e**, **8e**, **12a**, and **13e** identified as tubulin destabilizers in the sea urchin embryo assay also affected cellular microtubule structure (Figure 4B,D−F). It should be noted that **5a** and **5e** precipitated from 10 mM stock solutions in DMSO, therefore the data pertinent to these molecules could not be accurately interpreted. Compound **4′a** (an aromatic analogue of **4a**) featuring low cytotoxicity failed to induce sea urchin embryo development alterations and to depolymerize cellular microtubules (Figure 4C). Surprisingly, compound **9e** that exhibited modest cytotoxicity without the disruption of interphase microtubules in A549 cells did show a considerable antimitotic tubulin destabilizing activity in the sea urchin assay. The effect could be attributed to a somewhat selective interaction of this molecule with spindle microtubules in the sea urchin blastomeres vs interphase microtubules in cultured cancer cells. Treatment with PT at 0.1 and 5 μM resulted in complete disassembly of cellular microtubules (data not shown).

Cell Cycle Analysis. The ability of selected 4-aza-PTs to interfere with A549 and Jurkat cell cycle progression was estimated by propidium iodide staining followed by flow cytometry analysis. In A549 cells, PT as well as its aza-analogues **4a**,**g** and **6e** caused G2/M cell cycle arrest, exhibiting EC_{50} values of 16.5 ± 0.35, 16.2 ± 0.71, 230 ± 7.07, and 119 ± 1.41 nM, respectively. Compound **4′a** failed to affect the cell cycle progression even at 50 μM concentration. Notably, all three cell-based assays ranked the tested molecules similarly. Cytotoxicity and microtubule dynamics effects of 4-aza-PTs decreased in the following order: **4a** > **6e** > **4g** ≫ **4′a**. In Jurkat cells, both **8e** and PT were potent G_2/M blockers as well. In contrast, etoposide caused a pronounced cell cycle arrest in G_0/G_1 phase (Figure 5).

Apoptosis-Inducing Activity. It has been well established that tubulin binding compounds interfere with the dynamics and structure of both mitotic spindle and interphase microtubules, eventually leading to cell death by apoptosis. However the link between microtubule alteration and respective intracellular mechanisms responsible for initiation of apoptotic events remains unclear.[50−52] Caspases (intracellular proteases) play a key role in the apoptotic response. Their activation by specific signals triggers proteolysis of cellular substrates thereby executing apoptotic events.[53] There are two

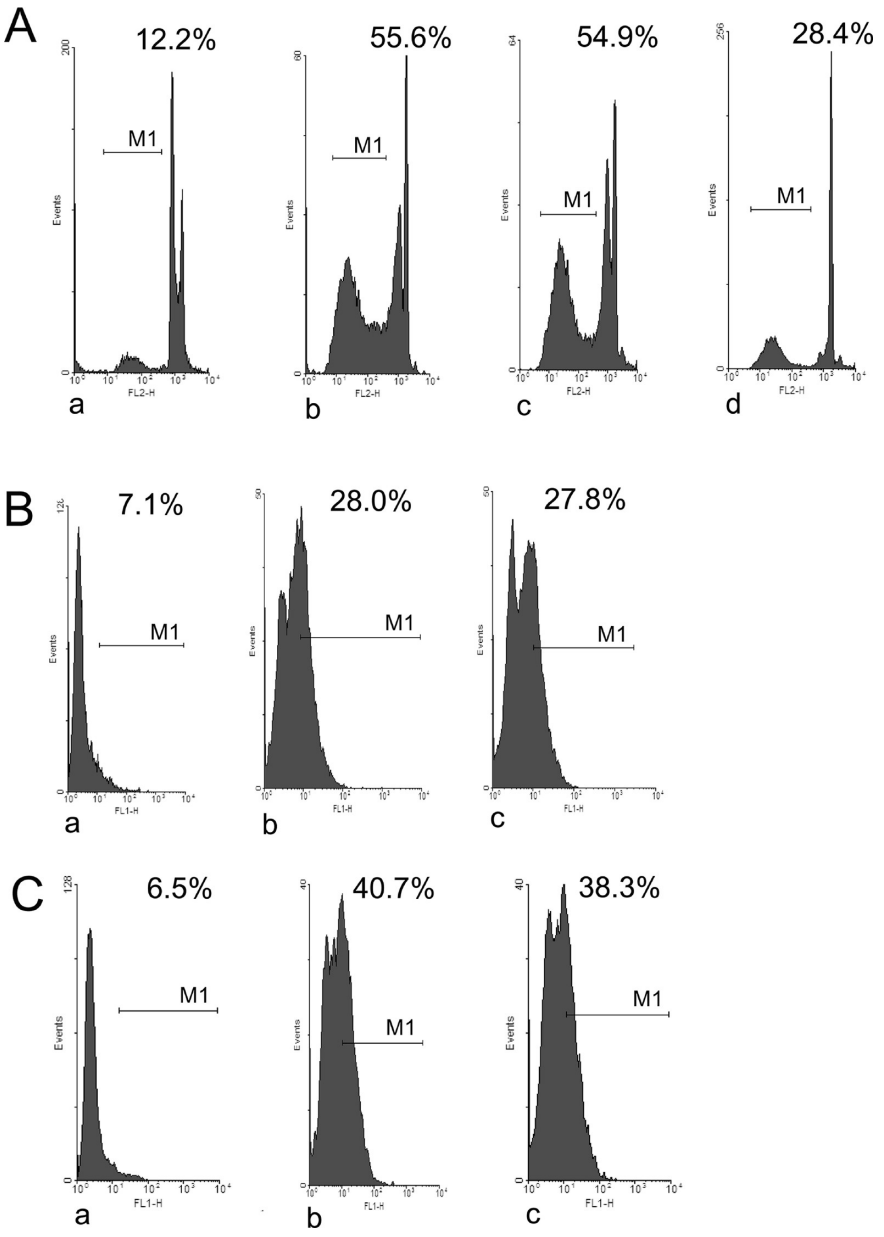

Figure 6. Jurkat cells treated with PT or **8e**: flow cytometry assessment of hypodyploid cells (A), cells with active form of caspase-3 (B), and with cleaved PARP (C). (a) Control (untreated cells); (b) PT, 50 nM, 48 h; (c) **8e**, 50 nM, 48 d. In (d), cells were pretreated with caspase inhibitor z-VAD-FMK (50 μM) for 2 h, followed by the incubation with **8e** as in (c). M1 comprises the hypodiploid cells (A), cells with active form of caspase-3 (B), and cleaved PARP-positive cells (C) with corresponding percentages given in each plot.

main apoptotic pathways, namely the extrinsic pathway that involves membrane-bound death receptors and leads to activation of caspase-8 and the mitochondria-related caspase-9-dependent intrinsic pathway. Both pathways converge onto the effector caspase-3 activated by the apical (initiator) caspases-8 and -9.[53,54] Caspase-2 combines both initiator and effector features.[53] Its processing requires caspase-9 and caspase-3.[55]

Generally, microtubule interfering agents induce caspase-dependent apoptotic cell death through intrinsic caspase-9-dependent pathway.[50−52,56] For instance, tubulin destabilizers combretastatin A-4 and its analogues, as well as nocodazole, trigger apoptosis through the intrinsic pathway accompanied by an activation of caspase-9 and caspase-3.[57−59] However, other tubulin-targeting compounds were found to induce apoptosis in human cancer cells via the activation of caspase-8 and -2 rather than caspase-9, suggesting the extrinsic pathway as a primary apoptotic mechanism.[60−63] Whether this difference is cell-specific or dependent on the compound remains unclear. Because numerous malignancies are characterized by molecular defects in the apoptotic pathways,[54] the investigation of apoptotic mechanisms is of particular importance.

There are a few data concerning the participation of effector caspases-3 and -7 in apoptosis caused by PT derivatives.[64−66] For 4-aza-PTs, caspase-3 activation in Jurkat and A549 cells has been described.[16,22,23] Up to now there is no evidence on the involvement of apical caspases-9 and -2 in cell death caused by PT derivatives. In the present study, the details of apoptosis induction by compound **4a** found to be the most cytotoxic against

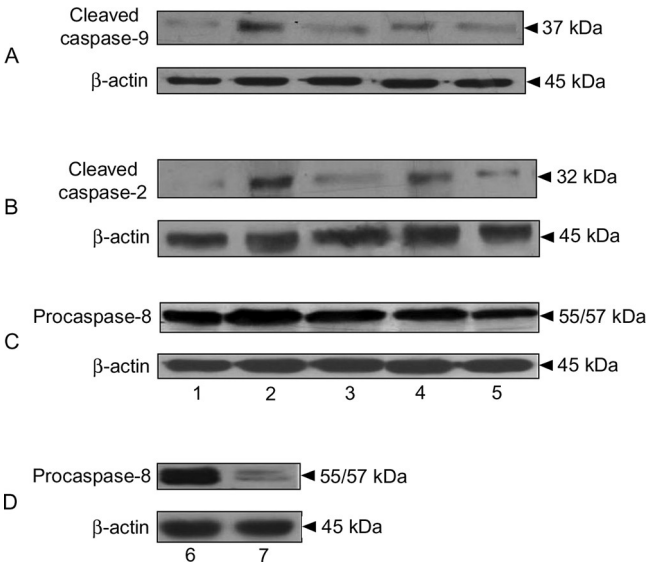

Figure 7. Western blot analysis of procaspase-8, cleaved caspase-2, and caspase-9 in total lysates of Jurkat cells. The lysates treated with PT or **8e** were prepared in SDS−Laemmli sample buffer. Immunoblotting was performed using monoclonal anticaspase-9 (A), anticaspase-2 (B), and antiprocaspase-8 (C, D) antibodies. β-Actin served as the loading control. Lanes: (1, 6) control (untreated cells); (2) PT, 50 nM, 24 h; (3) PT, 50 nM, 48 h; (4) **8e**, 50 nM, 24 h; (5) **8e**, 50 nM, 48 h; (7) etoposide, 2 μM, 24 h.

A549 cells, and **8e**, the most potent in the sea urchin embryo assay, were studied in A549 and Jurkat cells, respectively.

The proapoptotic activity of compound **8e** was examined in Jurkat cells. Apoptosis induction, cell cycle distribution, expression of active effector caspase-3 in cells, and cleavage of PARP were assessed quantitatively by flow cytometry. Procaspase-8 and the active form of apical caspase-2 and -9 were analyzed by Western blot. As evidenced by the flow cytometric assay, after 48 h, both **8e** and PT increased the hypodiploid subpopulation peak (sub-G1) indicative of apoptosis from 12% (control) to 55% of the total cell population (Figure 6A). To confirm the involvement of caspases in the **8e**-induced Jurkat cell death, an effect of pan-caspase inhibitor Z-VAD-fmk[67] has been examined. Jurkat cells were preincubated with Z-VAD-fmk at 50 μM for 2 h, followed by incubation with 50 nM of **8e** for additional 48 h. Pretreatment with Z-VAD-fmk decreased the content of apoptotic cells from 55% to 28% (Figure 6A), suggesting that cell death induced by **8e** was related to caspase activation. Approximately 30% of cells treated with **8e** or PT possessed active form of caspase-3, as compared to 7% in untreated cells (Figure 6B). Cleaved PARP, the product resulting from caspase-3 activation, has been identified in ca. 40% of the cells treated by **8e** or PT (Figure 6C).

Activation of caspases-9, -2, and -8 in cells treated with **8e** was further analyzed by Western blot. The exposure of Jurkat cells to **8e** resulted in the processing of procaspase-9 and -2, as evidenced by the appearance of their active forms (Figure 7A,B). The intensities of bands corresponding to active forms of caspase-9 and -2 upon 24 h of treatment with **8e** or PT were higher than those at 48 h, while the intensity of procaspase-8 55/57 kDa traces was unaltered (Figure 7C), suggesting lack of active caspase-8. As expected, etoposide caused the reduction of procaspase-8 level in Jurkat cells (Figure 7D).[68]

Finally, the ability of compound **4a** to trigger apoptotic and necrotic events in A549 cells was analyzed using double staining with Annexin V−FITC and 7-AAD (7-amino actinomycin D) dyes. The procedure allows for the differentiation between living (intact) (Annexin V−FITC$^-$/7-ADD$^-$), early apoptotic (Annexin V−FITC$^+$/7-ADD$^-$), late apoptotic (Annexin V−FITC$^+$/7-ADD$^+$), and necrotic cells (Annexin V−FITC$^-$/7-ADD$^+$).[69,70] Compound **4a** as well as nocodazole (positive control) induced a significant increase of early apoptosis and to a lesser degree necrosis without affecting late apoptosis (Figure S2, Supporting Information). The effects of **4a** were concentration-independent, suggesting that this compound might trigger apoptosis and necrosis even at lower concentrations. **4a** was more potent apoptotis- and necrosis-inducing agent than nocodazole.

On the basis of these data, we concluded that compounds **4a** and **8e** caused G2/M cell cycle arrest and apoptotic response in A549 and Jurkat human cancer cells, notably, that in Jurkat cells **8e** as well as PT induced caspase-dependent apoptosis mediated by the apical caspases-2 and -9 and not caspase-8, implying the involvement of the intrinsic caspase-9-dependent apoptotic pathway.

PT-Related Compounds: Mode of Action. In the sea urchin embryo assay, death of arrested eggs exposed to tubulin destabilizing agents was observed after 6−8 h of treatment with a test article. It has been suggested that apoptosis never occurs during sea urchin embryo cleavage, first appearing only at blastula stage just before hatching.[71] This explains the absence of quick cell division arrest and death at cleavage after treatment by various DNA-targeting agents known to trigger apoptosis such as etoposide, aloe-emodin, apigenin, 5-fluorouracil, and 4-phenylbutyric acid.[31] Correspondingly, the formation of multinucleated cells (Figure 1B) typical of tubulin destabilizers is an inherent morphological characteristic of mitotic catastrophe, a cell death different from apoptosis.[72]

Tubulin destabilizers including colchicine, nocodazole, combretastatins, phenstatin, indibulin, dolastatin 15, vinblastin, and others interacting with different binding sites on tubulin caused embryo spinning when applied at the swimming blastula stage. Spinning continued for several hours, followed by slow movements near the bottom of the vessel suggesting embryo viability.[31,33,34,73] In contrast, PT and some of 4-aza-PTs (**4a**,**e**,**g**,**j**, **6e**, **7e**, **8e**,**h**, **12a**, and **13e**) induced sea urchin embryo disintegration and death after spinning independently of compound concentration, probably owing to yet another microtubule-unrelated effect. In addition, compound **14′e** caused cleavage alteration at 100 nM, whereas it failed to produce cleavage arrest and embryo spinning, suggesting nontubulin antuproliferative activity. Similarly, **9e** exerted cytotoxic effect against A549 cells without microtubule disruption (Table 1). These results are correlated well with the reported ability of PT derivatives to induce cell death and sub-G1 apoptotic cell accumulation without cell cycle arrest and interphase microtubule damage.[10,14] Moreover, in a series of 4-aza-PTs with hetero aryl or benzo hetero aryl system instead of the A and B rings, chemical modifications of the ring E resulted in a significant decrease of antitubulin activity and retention of cytotoxicity.[22] A combination of our results and literature data suggests an alternative tubulin-independent mechanism of 4-aza-PTs embryotoxicity that could be evident at postcleavage stages of the sea urchin embryo development.

■ CONCLUSIONS

In conclusion, we synthesized a series of 4-aza-PT analogues from the easily accessible plant-derived polyalkoxybenzenes. A developed reaction sequence allows for an expedited synthesis

of the targeted molecules in 12−86% overall yields from naturally occurring building blocks. The resulting compounds were extensively evaluated in both phenotypic sea urchin embryo and cellular assays linking their observed cytotoxicity to a potent antimitotic tubulin destabilizing effect. Notably, the phenotypic sea urchin embryo assay allowed for rapid and reproducible identification of antitubulin molecules. These compounds were further reconfirmed as potent antimitotic agents by a panel of conventional cell-based assays. The most potent representative in each structural group featured myristicin-derived ring E (**4e**, **6e**, **8e**, **11e**, and **13e**), as evidenced by the in vivo sea urchin embryo assay. The activity of these new compounds compares favorably to the reported antimitotic agents containing myristicin-derived pharmacophore including corresponding phenstatin analogue and combretastatin A-2.[25,73] The ring B modification yielded 6-methoxy substituted molecule **8e** as the most active compound. Compound **4a** featuring 3,4,5- trimethoxybenzene substituent was the most cytotoxic against A549 human lung epithelial carcinoma cells, being more potent than the parent PT. The activity of 4-aza-PT derivatives correlated well between the sea urchin phenotypic and conventional cell-based assays. In Jurkat cells, both **8e** and PT induced caspase-dependent apoptosis mediated by the apical caspases-2 and -9 and not caspase-8, implying the involvement of the intrinsic caspase-9-dependent apoptotic pathway. The structure−activity data reported in this paper warrant further synthetic studies and biological evaluation of novel heterocyclic myristicine derivatives. Four specific molecules (**4e**, **7e**, **8e**, and **8h**) have been selected for advanced NCI60 human tumor cell line anticancer drug screen. Their antiproliferative activity will be reported separately.

EXPERIMENTAL SECTION

Chemistry. Materials and Methods. NMR spectra were collected on a Bruker DR-500 instrument [working frequencies of 500.13 MHz (^{1}H) and 75.47 (^{13}C)]. Mass spectra were obtained on a Finnigan MAT/INCOS 50 instrument (70 eV) using direct probe injection. Elemental analysis was accomplished with the automated Perkin-Elmer 2400 CHN microanalyzer. HPLC was performed using a Laboratorni Pristroje (Praha, Czech Republic) chromatograph. Ozonolysis was conducted using a custom-designed apparatus (Science and Technology Park, St. Petersburg State Polytechnic University, Russia) equipped with an IR detector of O_3 concentration (Japan) and an automated shutdown circuit. The device allowed for the controlled generation of ozone, with a maximal capacity of 10 g of O_3 per h from O_2. The compound purity has been determined by NMR, HPLC, and elemental analyses. Purity of compounds **4′**−**15′**, **4**−**13**, and **17**−**19** was determined to be ≥95%.

Isolation of Plant Allylpolyalkoxybenzenes[24]. Liquid CO_2 extraction of parsley and dill seeds was carried out earlier by Company Karavan Ltd. (Krasnodar, Russia). Allylpolymethoxybenzenes **1b**−**e** with 98−99% purity were obtained by high-efficiency distillation using a pilot plant device at N. D. Zelinsky Institute of Organic Chemistry, RAS (Moscow, Russia). The seed essential oils of parsley varieties cultivated in Russia contained 70−75% of **1b** (var. Sakharnaya), 21% of **1d** (var. Slavyanovskaya), and 40−46% of **1e** (var. Astra). Indian dill seeds were purchased from Vremya & Co. (St. Petersburg, Russia). The dill seed essential oil contained 30−33% of **1c**.

General Procedure A for the Synthesis of Quinolines 4′−15′[36]. A solution of aromatic amine (50 mmol), ethyl 4-chloroacetoacetate (50 mmol) and acetic acid (3 mL) in 100 mL of benzene was refluxed for 8 h. The reaction mixture was cooled to room temperature, and the precipitated product was collected by vacuum filtration and washed with EtOH (30 mL). In most cases, the resulting products **3** were obtained with >85% purity as judged by NMR analysis. A solution of corresponding anilinolactone **3** (2 mmol), appropriate aromatic aldehyde (**2a**−**k**) (2.2 mmol), and *p*-chloranil (2 mmol) in TFA (3 mL) was stirred at room temperature for 24 h. The reaction mixture was quenched with water (50 mL) and extracted with CH_2Cl_2 (3 × 20 mL). The organic layers were combined, washed with 5% $NaHCO_3$ (2 × 20 mL), water (2 × 20 mL), dried over anhydrous sodium sulfate, and concentrated in vacuum to obtain the crude product. Flash chromatography purification (petroleum ether/EtOAc, 4:1−1:1) afforded targeted quinolines **4′**−**15′** as a white solid.

General Procedure B for the Synthesis of 4-Aza-podophyllotoxin Derivatives 4−13. A suspension of quinoline **4′**−**13′** (0.26 mmol) in a glacial AcOH (3.96 mmol, 3 mL) was treated with $NaBH_3CN$ (0.78 mmol), and the resulting mixture was stirred for 3 h at room temperature and treated with the ice water (15 mL). The precipitate was filtered, washed with ethanol (2 × 1 mL), and the product was purified by column chromatography (petroleum ether/EtOAc, 2:1) to afford the targeted 4-aza-podophyllotoxins **4**−**13** as a white solid. NMR analysis confirmed the absence of intermediates **4′**−**13′**.

General Procedure C for the Synthesis of Dihydropyridopyrazole Derivatives 17−19. A mixture of of corresponding pyrazole (1 mmol), tetronic acid **16** (1 mmol), triethylamine (0.05 mL), and appropriate aldehyde (**2a**−**k**) (1 mmol) in EtOH (5 mL) was refluxed for 3 h. The reaction mixture was cooled to +4 °C, and the precipitated product was collected by vacuum filtration and washed with EtOH (2 mL) at 0 °C. Purification by flash chromatography (petroleum ether/EtOAc, 4:1−2:1) afforded the targeted 4-aza-dihydropodophyllotoxins **17**−**19** as a white solid.

Synthetic and Analytical Data for Selected 4-Aza-podophyllotoxins. Data for the other compounds are presented in Supporting Information.

9-(6,7-Dimethoxy-1,3-benzodioxol-5-yl)[1,3]dioxolo[4,5-*g*]furo[3,4-*b*]quinolin-8(6*H*)-one (4′c). The title compound was obtained according to the general procedure A. Yield 27%, mp 241−244 °C. ^{1}H NMR (DMSO-d_6): δ 3.35 (s, 3H, OCH_3-6′), 4.02 (s, 3H, OCH_3-7′), 5.42 (d, J = 15.4 Hz, 1H, OCH_2-6), 5.49 (d, J = 15.4 Hz, 1H, OCH_2-6), 6.11 and 6.13 (s, 2H, OCH_2O-2′), 6.28 (s, 2H, OCH_2O-2), 6.51 (s, 1H, H-4′), 6.89 (s, 1H, H-10), 7.52 (s, 1H, H-4). EIMS m/z 409 $[M]^+$ (25), 394 (1), 351 (15), 350 (68), 224 (23), 167 (100). Anal. Calcd for $C_{21}H_{15}NO_8$: C, 61.62; H, 3.69; N, 3.42. Found: C, 61.69; H, 3.72; N, 3.36.

9-(6,7-Dimethoxy-1,3-benzodioxol-5-yl)-6,9-dihydro-[1,3]dioxolo[4,5-*g*]furo[3,4-*b*]quinolin-8(5*H*)-one (4c). The title compound was obtained according to the general procedure B. Yield 26%, mp 295−298 °C. ^{1}H NMR (DMSO-d_6): δ 3.73 (s, 3H, OCH_3-6′), 3.94 (s, 3H, OCH_3-7′), 4.83 (d, J = 15.6 Hz, 1H, OCH_2-6), 4.95 (d, J = 15.7 Hz, 1H, OCH_2-6), 5.13 (s, 1H, H-9), 5.88 and 5.94 (s, 2H, OCH_2O-2), 5.89 and 5.91 (s, 2H, OCH_2O-2′), 6.24 (s, 2H, H-4′), 6.42 (s, 1H, H-10), 6.49 (s, 1H, H-4), 9.81 (s, 1H, NH-5). EIMS m/z 411 $[M]^+$ (20), 380 (100), 366 (17), 230 (39), 172 (7). Anal. Calcd for $C_{21}H_{17}NO_8$: C, 61.32; H, 4.17; N, 3.40. Found: C, 61.29; H, 4.14; N, 3.44.

9-(7-Methoxy-1,3-benzodioxol-5-yl)-6,9-dihydro[1,3]dioxolo[4,5-*g*]furo[3,4-*b*]quinolin-8(5*H*)-one (4e). The title compound was obtained according to the general procedure B. Yield 55%, mp 308−310 °C. ^{1}H NMR (DMSO-d_6): δ 3.80 (s, 3H, OCH_3-7′), 4.83 (s, 1H, H-9), 4.84 (d, J = 15.7 Hz, 1H, OCH_2-6), 4.97 (d, J = 15.7 Hz, 1H, OCH_2-6), 5.90 and 5.91 (s, 2H, OCH_2O-2′), 5.90 and 5.96 (s, 2H, OCH_2O-2), 6.33 (d, J = 1.4 Hz, 1H, H-4′), 6.52 (s, 1H, H-10), 6.56 (d, J = 1.4 Hz, 1H, H-6′), 6.64 (s, 1H, H-4), 9.87 (s, 1H, NH-5). EIMS m/z 381 $[M]^+$ (5), 231 (14), 230 (100), 152 (24), 151 (7). Anal. Calcd

for $C_{20}H_{15}NO_7$: C, 62.99; H, 3.96; N, 3.67. Found: C, 63.06; H, 4.03; N, 3.60.

9-Phenyl-6,9-dihydro[1,3]dioxolo[4,5-*g*]furo[3,4-*b*]quinolin-8(5*H*)-one (4k). The title compound was obtained according to the general procedure B. Yield 73%, mp 290−293 °C (lit.[6] mp 295−298 °C). ^{1}H NMR (DMSO-d_6): δ 4.85 (d, J = 15.7 Hz, 1H, OCH_2-6), 4.91 (s, 1H, H-9), 4.94 (d, J = 15.7 Hz, 1H, OCH_2-6), 5.89 and 5.95 (s, 2H, OCH_2O-2), 6.53 (s, 1H, H-10), 6.56 (s, 1H, H-4), 7.15 (t, J = 7.2 Hz, 1H, H-4′), 7.19 (d, J = 7.2 Hz, 2H, H-2′,6′), 7.26 (d, J = 7.2 Hz, 2H, H-3′,5′), 9.87 (s, 1H, NH-5). EIMS m/z 307 $[M]^+$ (20), 230 (21), 78 (12), 77 (100). Anal. Calcd for $C_{18}H_{13}NO_4$: C, 70.35; H, 4.26; N, 4.56. Found: C, 70.29; H, 4.22; N, 4.63.

10-Methoxy-9-(7-methoxy-1,3-benzodioxol-5-yl)-6,9-dihydro[1,3]dioxolo[4,5-*g*]furo[3,4-*b*]quinolin-8(5*H*)-one (5e). The title compound was obtained according to the general procedure B. Yield 26%, mp 321−326 °C. ^{1}H NMR (DMSO-d_6): δ 3.66 (s, 3H, OCH_3-10), 3.77 (s, 3H, OCH_3-7′), 4.78 (d, J = 15.7 Hz, 1H, OCH_2-6), 4.89 (d, J = 15.7 Hz, 1H, OCH_2-6), 4.89 (s, 1H, H-9), 5.89 and 5.96 (s, 2H, OCH_2O-2), 5.89 and 5.90 (s, 2H, OCH_2O-2′), 6.22 (d, J = 1.4 Hz, 1H, H-4′), 6.33 (s, 1H, H-4), 6.42 (d, J = 1.4 Hz, 1H, H-6′), 9.93 (s, 1H, NH-5). EIMS m/z 411 $[M]^+$ (3), 384 (0.5), 260 (100), 245 (25), 152 (31), 151 (9). Anal. Calcd for $C_{21}H_{17}NO_8$: C, 61.32; H, 4.17; N, 3.40. Found: C, 61.36; H, 4.18; N, 3.38.

6-Methoxy-9-(7-methoxy-1,3-benzodioxol-5-yl)-4,9-dihydrofuro[3,4-*b*]quinolin-1(3*H*)-one (8e). The title compound was obtained according to the general procedure B. Yield 60%, mp 278−280 °C. ^{1}H NMR (DMSO-d_6): δ 3.70 (s, 3H, OCH_3-6), 3.80 (s, 3H, OCH_3-7′), 4.84 (d, J = 15.5 Hz, 1H, OCH_2-3), 4.86 (s, 1H, H-9), 4.97 (d, J = 15.5 Hz, 1H, OCH_2-3), 5.89 and 5.90 (s, 2H, OCH_2O-2′), 6.31 (d, J = 1.4 Hz, 1H, H-4′), 6.44 (d, J = 2.5 Hz, H-5), 6.52 (dd, J = 8.6, 2.5 Hz, 1H, H-7), 6.53 (d, J = 1.4 Hz, 1H, H-6′), 6.99 (d, J = 8.6 Hz, H-8), 9.94 (s, 1H, NH-4). EIMS m/z 367 $[M]^+$ (14), 217 (15), 216 (100), 152 (16), 151 (7). Anal. Calcd for $C_{20}H_{17}NO_6$: C, 65.39; H, 4.66; N, 3.81. Found: C, 65.42; H, 4.69; N, 3.74.

9-(3,5-Dimethoxyphenyl)-6-methoxy-4,9-dihydrofuro-[3,4-*b*]quinolin-1(3*H*)-one (8h). The title compound was obtained according to the general procedure B. Yield 43%, mp 229−233 °C (lit.[6] mp 254 °C). ^{1}H NMR (DMSO-d_6): δ 3.68 (s, 6H, 2 × OCH_3-3′, 5′), 3.70 (s, 3H, OCH_3-6), 4.85 (d, J = 15.8 Hz, 1H, OCH_2-3), 4.85 (s, 1H, H-9), 4.98 (d, J = 15.8 Hz, 1H, OCH_2-3), 6.30 (t, J = 2.2 Hz, 1H, H-4′), 6.32 (d, J = 2.2 Hz, 2H, H-2′,6′), 6.45 (d, J = 2.6 Hz, H-5), 6.52 (dd, J = 8.5, 2.6 Hz, 1H, H-7), 6.99 (d, J = 8.5 Hz, H-8), 9.94 (s, 1H, NH-4). EIMS m/z 353 $[M]^+$ (12), 217 (15), 216 (100), 138 (16). Anal. Calcd for $C_{20}H_{19}NO_5$: C, 67.98; H, 5.42; N, 3.96. Found: C, 67.91; H, 5.38; N, 4.04.

4-(4,7-Dimethoxy-1,3-benzodioxol-5-yl)-3-methyl-1,4,7,8-tetrahydro-5*H*-furo[3,4-*b*]pyrazolo[4,3-*e*]pyridin-5-one (18b). The title compound was obtained according to the general procedure C. Yield 47%, mp 295−297 °C. ^{1}H NMR (DMSO-d_6): δ 1.83 (s, 3H, CH_3-3), 3.69 (s, 3H, OCH_3-4′), 3.71 (s, 3H, OCH_3-7′), 4.78 (d, J = 15.7 Hz, 1H, OCH_2-7), 4.85 (d, J = 15.7 Hz, 1H, OCH_2-7), 4.99 (s, 1H, H-4), 5.98 and 5.99 (s, 2H, OCH_2O-2′), 6.23 (s, 1H, H-6′), 10.03 (s, 1H, NH-8), 11.79 (s, 1H, NH-1). EIMS m/z 371 $[M]^+$ (31), 341 (14), 340 (74), 327 (5), 326 (21), 312 (16), 296 (14), 191 (11), 190 (100), 182 (10). Anal. Calcd for $C_{18}H_{17}N_3O_6$: C, 58.22; H, 4.61; N, 11.32. Found: C, 58.30; H, 4.68; N, 11.23.

Biology. Materials and Methods. Sea Urchin Embryo Assay. Adult sea urchins *Paracentrotus lividus* were collected from the Mediterranean Sea at the Cyprus coast and kept in an aerated seawater tank. Gametes were obtained by intracoelomic injection of 0.5 M KCl. Eggs were washed with filtered seawater and fertilized by adding drops of a diluted sperm. Embryos were cultured at room temperature under gentle agitation with a motor-driven plastic paddle (60 rpm) in filtered seawater. The embryos were observed with a light microscope Biolam (LOMO, S.-Petersburg, Russia). For treatment with the test compounds, 5 mL aliquots of embryo suspension were transferred to 6-well plates and incubated as a monolayer at a concentration up to 2000 embryos/mL. Stock solutions of compounds were prepared in DMSO at 5−10 mM concentrations, followed by a 10-fold dilution with 95% EtOH. This procedure enhanced solubility of the test compounds in the salt-containing medium (seawater), as evidenced by microscopic examination of the samples. The maximal tolerated concentrations of DMSO and EtOH in the in vivo assay were determined to be 0.05% and 1% respectively. Higher concentrations of either DMSO (≥0.1%) or EtOH (>1%) caused nonspecific alteration and retardation of the sea urchin embryo development independent of the treatment stage. Podophyllotoxin (Aldrich) and topoisomerase II inhibitor etoposide (LANS, Veropharm, Russia, 20 mg/mL in 96% EtOH) served as reference compounds.

The antiproliferative activity was assessed by exposing fertilized eggs (8−20 min after fertilization, 43−55 min before the first mitotic cycle completion) to 2-fold decreasing concentrations of the compound. Cleavage alteration and arrest were clearly detected at 2.5−5.5 h after fertilization. The effects were quantitatively estimated as a threshold concentration resulting in cleavage alteration and embryo death before hatching or full mitotic arrest. At these concentrations, all tested tubulin destabilizers caused 100% cleavage alteration and embryo death before hatching, whereas at 2-fold lower concentrations, the compounds failed to produce any effect. For tubulin destabilizing activity, the compounds were tested on free-swimming blastulae just after hatching (9−10 h after fertilization), originated from the same embryo culture. Embryo spinning was observed after 15 min to 20 h of treatment, depending on the nature and concentration of the compound. Both spinning and lack of forward movement were interpreted to be the result of the tubulin destabilizing activity of a molecule according to previous studies.[31] Video illustrations are available at http://www.chemblock.com). Compound substructure search in sea urchin embryo screening database is available free online at http://www.zelinsky.ru.

■ ASSOCIATED CONTENT

Supporting Information. Effects of compounds 4′−15′ and **17**−**19** on the sea urchin embryo development, experimental details regarding syntheses and analytical data, biological assay methods. This material is available free of charge via the Internet at http://pubs.acs.org.

■ AUTHOR INFORMATION

Corresponding Author

*Phone: +7 (916) 620-9584. Fax: +7 (499) 137-2966. E-mail: vs@zelinsky.ru.

■ ACKNOWLEDGMENT

This work was supported by Alexander von Humboldt Foundation (no. 3.4-Fokoop-Rus/1015567, Germany) and a grant from Chemical Block Ltd.

■ ABBREVIATIONS USED

PT, podophyllotoxin; SAR, structure−activity relationship; 7-AAD, 7-amino actinomycin D; PARP, poly ADP-ribose polymerase

■ REFERENCES

(1) Ravelli, R. B. G.; Gigant, B.; Curmi, P. A.; Jourdain, I.; Lachkar, S.; Sobel, A.; Knossow, M. Insight into tubulin regulation from a complex with colchicine and a stathmin-like domain. *Nature* **2004**, *428*, 198–202.

(2) Gupta, S.; Das, L.; Datta, A. B.; Poddar, A.; Janik, M. E.; Bhattacharyya, B. Oxalone and lactone moieties of podophyllotoxin exhibit properties of both the B and C rings of colchicine in its binding with tubulin. *Biochemistry* **2006**, *45*, 6467–6475.

(3) Desbene, S.; Giorgi-Renault, S. Drugs that inhibit tubulin polymerization: The particular case of podophyllotoxin and analogues. *Curr. Med. Chem.: Anti-Cancer Agents* **2002**, *2*, 71–90.

(4) Chen, S.-W.; Wang, Y.-H.; Jin, Y.; Tian, X.; Zheng, Y.-T.; Luo, D.-Q.; Tu, Y.-Q. Synthesis and anti-HIV-1 activities of novel podophyllotoxin derivatives. *Bioorg. Med. Chem. Lett.* **2007**, *17*, 2091–2095.

(5) Saitoh, T.; Kuramochi, K.; Imai, T.; Takata, K.; Takehara, M.; Kobayashi, S.; Sakaguchia, K.; Sugawara, F. Podophyllotoxin directly binds a hinge domain in E2 of HPV and inhibits an E2/E7 interaction in vitro. *Bioorg. Med. Chem.* **2008**, *16*, 5815–5825.

(6) Frackenpohl, J.; Adelt, I.; Antonicek, H.; Arnold, C.; Behrmann, P.; Blaha, N.; Böhmer, J.; Gutbrod, O.; Hanke, R.; Hohmann, S.; van Houtdreve, M.; Losel, P.; Malsam, O.; Melchers, M.; Neufert, V.; Peschel, E.; Reckmann, U.; Schenke, T.; Thiesen, H.-P.; Velten, R.; Vogelsang, K.; Weiss, H.-C. Insecticidal heterolignans—tubuline polymerization inhibitors with activity against chewing pests. *Bioorg. Med. Chem.* **2009**, *17*, 4160–4184.

(7) Xu, H.; Lv, M.; Tian, X. A review on hemisynthesis, biosynthesis, biological activities, mode of action, and structure−activity relationship of podophyllotoxins: 2003−2007. *Curr. Med. Chem.* **2009**, *16*, 327–349.

(8) Xu, H.; Xiao, X. Natural products-based insecticidal agents 4. Semisynthesis and insecticidal activity of novel esters of 2-chloropodophyllotoxin against *Mythimna separata* Walker in vivo. *Bioorg. Med. Chem. Lett.* **2009**, *19*, 5415–5418.

(9) Xu, H.; He, X.-Q. Natural products-based insecticidal agents 6. Design, semisynthesis, and insecticidal activity of novel monomethyl phthalate derivatives of podophyllotoxin against *Mythimna separata* Walker in vivo. *Bioorg. Med. Chem. Lett.* **2010**, *20*, 4503–4506.

(10) Damayanthi, Y.; Lown, J. W. Podophyllotoxins: current status and recent developments. *Curr. Med. Chem.* **1998**, *5*, 205–252.

(11) Canel, C.; Moraes, R. M.; Dayan, F. E.; Ferreira, D. Podophyllotoxin. *Phytochemistry* **2000**, *54*, 115–120.

(12) Meresse, P.; Dechaux, E.; Monneret, C.; Bertounesque, E. Etoposide: discovery and medicinal chemistry. *Curr. Med. Chem.* **2004**, *11*, 2443–2466.

(13) Duca, M.; Guianvarc'h, D.; Meresse, P.; Bertounesque, E.; Dauzonne, D.; Kraus-Berthier, L.; Thirot, S.; Leonce, S.; Pierre, A.; Pfeiffer, B.; Renard, P.; Arimondo, P. B.; Monneret, C. Synthesis and biological study of a new series of 4′-demethylepipodophyllotoxin derivatives. *J. Med. Chem.* **2005**, *48*, 593–603.

(14) Castro, M. A.; del Corral, J. M. M.; Garcia, P. A.; Rojo, M. V.; de la Iglesia-Vicente, J.; Mollinedo, F.; Cuevas, C.; San Feliciano, A. Synthesis and biological evaluation of new podophyllic aldehyde derivatives with cytotoxic and apoptosis-inducing activities. *J. Med. Chem.* **2010**, *53*, 983–993.

(15) Magedov, I. V.; Manpadi, M.; Rozhkova, E.; Przheval'skii, N. M.; Rogelj, S.; Shors, S. T.; Steelant, W. F.; Van Slambrouck, S.; Kornienko, A. Structural simplification of bioactive natural products with multicomponent synthesis: dihydropyridopyrazole analogues of podophyllotoxin. *Bioorg. Med. Chem. Lett.* **2007**, *17*, 1381–1385.

(16) Magedov, I. V.; Manpadi, M.; Slambrouck, S. V.; Steelant, W. F.; Rozhkova, E.; Przheval'skii, N. M.; Rogelj, S.; Kornienko, A. Discovery and investigation of antiproliferative and apoptosis-inducing properties of new heterocyclic podophyllotoxin analogues accessible by a one-step multicomponent synthesis. *J. Med. Chem.* **2007**, *50*, 5183–5192.

(17) Shi, C.; Wang, J.; Chen, H.; Shi, D. Regioselective synthesis and in vitro anticancer activity of 4-aza-podophyllotoxin derivatives catalyzed by L-proline. *J. Comb. Chem.* **2010**, *12*, 430–434.

(18) Hitotsuyanagi, Y.; Kobayashi, M.; Morita, H.; Itokawa, H.; Takeya, K. Synthesis of (−)-4-aza-4-deoxypodophyllotoxin from (−)-podophyllotoxin. *Tetrahedron Lett.* **1999**, *40*, 9107–9110.

(19) Hitotsuyanagi, Y.; Fukuyo, M.; Tsuda, K.; Kobayashi, M.; Ozeki, A.; Itokawa, H.; Takeya, K. 4-Aza-2,3-dehydro-4-deoxypodophyllotoxins: simple aza-podophyllotoxin analogues possessing potent cytotoxicity. *Bioorg. Med. Chem. Lett.* **2000**, *10*, 315–317.

(20) Husson, H.-P.; Giorgi-Renault, S.; Tratrat, C.; Atassi, G.; Pierre, A.; Renard, P.; Pfeiffer, B. Dihydrofuro[3,4-*b*]quinolin-1-one compounds. U.S. Patent 6,548,515, 2003.

(21) Labruere, R.; Gautier, B.; Testud, M.; Seguin, J.; Lenoir, C.; Desbene-Finck, S.; Helissey, P.; Garbay, C.; Chabot, G. G.; Vidal, M.; Giorgi-Renault, S. Design, synthesis, and biological evaluation of the first podophyllotoxin analogues as potential vascular-disrupting agents. *ChemMedChem.* **2010**, *5*, 2016–2025.

(22) Kamal, A.; Suresh, P.; Mallareddy, A.; Kumar, B. A.; Reddy, P. V.; Raju, P.; Tamboli, J. R.; Shaik, T. B.; Jain, N.; Kalivendi, S. V. Synthesis of a new 4-aza-2,3-didehydropodophyllotoxin analogues as potent cytotoxic and antimitotic agents. *Bioorg. Med. Chem.* **2011**, *19*, 2349–2358.

(23) Magedov, I. V.; Frolova, L.; Manpadi, M.; Bhoga, U. D.; Tang, H.; Evdokimov, N. M.; George, O.; Georgiou, K. H.; Renner, S.; Getlik, M.; Kinnibrugh, T. L.; Fernandes, M. A.; van Slambrouck, S.; Steelant, W. F. A.; Shuster, C. B.; Rogelj, S.; van Otterlo, W. A. L.; Kornienko, A. Anticancer properties of an important drug lead podophyllotoxin can be efficiently mimicked by diverse heterocyclic scaffolds accessible via one-step synthesis. *J. Med. Chem.* **2011**, *54*, 4234–4246.

(24) Semenov, V. V.; Rusak, V. A.; Chartov, E. M.; Zaretsky, M. I.; Konyushkin, L. D.; Firgang, S. I.; Chizhov, A. O.; Elkin, V. V.; Latin, N. N.; Bonashek, V. M.; Stas'eva, O. N. Polyalkoxybenzenes from plant raw materials 1. Isolation of polyalkoxybenzenes from CO_2 extracts of *Umbelliferae* plant seeds. *Russ. Chem. Bull.* **2007**, *56*, 2448–2455.

(25) Semenov, V. V.; Kiselyov, A. S.; Titov, I. Y.; Sagamanova, I. K.; Ikizalp, N. N.; Chernysheva, N. B.; Tsyganov, D. V.; Konyushkin, L. D.; Firgang, S. I.; Semenov, R. V.; Karmanova, I. B.; Raihstat, M. M.; Semenova, M. N. Synthesis of antimitotic polyalkoxyphenyl derivatives of combretastatin using plant allylpolyalkoxybenzenes. *J. Nat. Prod.* **2010**, *73*, 1796–1802.

(26) (a) Petcher, T. J.; Weber, H. P.; Kuhn, M.; Von Wartburg, A. Crystal structure and absolute configuration of 2′-bromopodophyllotoxin-0.5 ethyl acetate. *J. Chem. Soc., Perkin Trans. 2* **1973**, *2*, 288–292. (b) Rithner, C. D.; Bushweller, C. H.; Gender, W. J.; Hoogasian, S. Dynamic nuclear magnetic resonance and empirical force field studies of podophyllotoxin. *J. Org. Chem.* **1983**, *48*, 1491–1495.

(27) Shulgin, A. T. *Tinkal: The Continuation*; Transform Press: Berkeley, CA, 1977; p 646.

(28) Lichius, J. J.; Thoison, O.; Montagnac, A.; Pais, M.; Gueritte-Voegelein, F.; Sevenet, T.; Cosson, J. P.; Hadi, A. H. Antimitotic and cytotoxic flavonols from *Zieridium pseudobtusifolium* and *Acronychia porteri*. *J. Nat. Prod.* **1994**, *57*, 1012–1016.

(29) Walle, T. Methoxylated flavones, a superior cancer chemopreventive flavonoid subclass? *Semin Cancer Biol.* **2007**, *17*, 354–362.

(30) Quintin, J.; Buisson, D.; Thoret, S.; Cresteil, T.; Lewin, G. Semisynthesis and antiproliferative evaluation of a series of 3′-aminoflavones. *Bioorg. Med. Chem. Lett.* **2009**, *19*, 3502–3506.

(31) Semenova, M. N; Kiselyov, A. S.; Semenov, V. V. Sea urchin embryo as a model organism for the rapid functional screening of tubulin modulators. *BioTechniques* **2006**, *40*, 765–774.

(32) Semenova, M. N.; Tsyganov, D. V.; Yakubov, A. P.; Kiselyov, A. S.; Semenov, V. V. A synthetic derivative of plant allylpolyalkoxybenzenes induces selective loss of motile cilia in sea urchin embryos. *ACS Chem. Biol.* **2008**, *3*, 95−100.

(33) Semenova, M. N.; Kiselyov, A. S.; Titov, I. Y.; Raihstat, M. M.; Molodtsov, M.; Grishchuk, E.; Spiridonov, I.; Semenov, V. V. In vivo evaluation of indolyl glyoxamides in the sea urchin embryo model: correlation with in vitro tubulin dynamics effects. *Chem. Biol. Drug Des.* **2007**, *70*, 485–490.

(34) Kiselyov, A. S.; Semenova, M. N.; Chernyshova, N. B.; Leitao, A.; Samet, A. V.; Kislyi, K. A.; Raihstat, M. M.; Oprea, T.; Lemcke, T.; Lantowe, M.; Weiss, D. G.; Ikizalp, N. N.; Kuznetsov, S. A.; Semenov, V. V. Novel derivatives of 1,3,4-oxadiazoles are potent mitostatic agents featuring strong microtubule depolymerizing activity in the sea urchin embryo and cell culture assays. *Eur. J. Med. Chem.* **2010**, *45*, 1683–1697.

(35) Schmidt, D. G.; Seemuth, P. D.; Zimmer, H. Substituted .gamma.-butyrolactones. Part 31. 2,4(3*H*,5*H*)-Furandione: heteroannulations with aromatic *o*-amino carbonyl compounds and condensations with some vic-polyones. *J. Org. Chem.* **1983**, *48*, 1914–1916.

(36) Hitotsuyanagi, Y.; Kobayashi, M.; Fukuyo, M.; Takeya, K.; Itokawa, H. A facile synthesis of the 4-aza-analogs of 1-arylnaphthalene lignans chinensin, justicidin B, and taiwanin C. *Tetrahedron Lett.* **1997**, *38*, 8295–8296.

(37) Tratrat, C.; Giorgi-Renault, S.; Husson, H.-P. A multicomponent reaction for the one-pot synthesis of 4-aza-2,3-didehydropodophyllotoxin and derivatives. *Org. Lett.* **2002**, *4*, 3187–3189.

(38) Ogiku, T.; Yoshida, S.; Ohmizu, H.; Iwasaki, T. Efficient syntheses of 1-arylnaphthalene lignan lactones and related compounds from cyanohydrins. *J. Org. Chem.* **1995**, *60*, 4585–4590.

(39) Cow, C.; Leung, C.; Charlton, J. L. Antiviral activity of arylnaphthalene and aryldihydronaphthalene lignans. *Can. J. Chem.* **2000**, *78*, 553–561.

(40) Ban, H. S.; Lee, S.; Kim, Y. P.; Yamaki, K.; Shin, K. H.; Ohuchi, K. Inhibition of prostaglandin E(2) production by taiwanin C isolated from the root of *Acanthopanax chiisanensis* and the mechanism of action. *Biochem. Pharmacol.* **2002**, *64*, 1345–1354.

(41) Chang, S.-T.; Sheng-Yang Wang, S.-Y.; Yueh-Hsiung Kuo, Y.-H. Resources and bioactive substances from Taiwania (*Taiwania cryptomerioides*). *J. Wood Sci.* **2003**, *49*, 1–4.

(42) Foley, P.; Eghbali, N.; Anastas, P. T. Silver-catalyzed one-pot synthesis of arylnaphthalene lactone natural products. *J. Nat. Prod.* **2010**, *73*, 811–813.

(43) Momose, T.; Toyooka, N.; Takeuchi, Y. A laboratory synthesis of 4-hydroxy-2(5*H*)-furanone (*β*-tetronic acid). *Heterocycles* **1986**, *24*, 1429–1431.

(44) Jin, Y.; Chen, S. W.; Tian, X. Synthesis and biological evaluation of new spin-labeled derivatives of podophyllotoxin. *Bioorg. Med. Chem.* **2006**, *14*, 3062–3068.

(45) Cisney, M. E.; Shilling, W. L.; Hearon, W. M.; Goheen, D. W. Conidendrin. II. The stereochemistry and reactions of the lactone ring. *J. Am. Chem. Soc.* **1954**, *76*, 5083–5087.

(46) Dantzig, A.; LaLonde, R. T.; Ramdayal, F.; Shepard, R. L.; Yanai, K.; Zhang, M. Cytotoxic responses to aromatic ring and configurational variations in alpha-conidendrin, podophyllotoxin, and sikkimotoxin derivatives. *J. Med. Chem.* **2001**, *44*, 180–185.

(47) Berkowitz, D. B.; Maeng, J.-H.; Dantzig, A. H.; Shepard, R. L.; Norman, B. H. Chemoenzymatic and ring E-modular approach to the (−)-podophyllotoxin skeleton. Synthesis of 3′,4′,5′-tridemethoxy-(−)-podophyllotoxin. *J. Am. Chem. Soc.* **1996**, *118*, 9426–9427.

(48) Goldbrunner, M.; Loidl, G.; Polossek, T.; Mannschreck, A.; von Angerer, E. Inhibition of tubulin polymerization by 5,6-dihydroindolo-[2,1-alpha]isoquinoline derivatives. *J. Med. Chem.* **1997**, *40*, 3524–3533.

(49) Mosmann, T. Rapid colorimetric assay for cellular growth and survival: application to proliferation and cytotoxicity assays. *J. Immunol. Methods* **1983**, *65*, 55–63.

(50) Bhalla, K. N. Microtubule-targeted anticancer agents and apoptosis. *Oncogene* **2003**, *22*, 9075–9086.

(51) Mollinedo, F.; Gajate, C. Microtubules, microtubule-interfering agents and apoptosis. *Apoptosis* **2003**, *8*, 413–450.

(52) Gascoigne, K. E.; Taylor, S. S. How do anti-mitotic drugs kill cancer cells? *J Cell Sci.* **2009**, *122*, 2579–2585.

(53) Pop, C.; Salvesen, G. S. Human caspases: activation, specificity, and regulation. *J. Biol. Chem.* **2009**, *284*, 21777–21781.

(54) Ghobrial, I. M.; Witzig, T. E.; Adjei, A. A. Targeting apoptosis pathways in cancer therapy. *Cancer J. Clin.* **2005**, *55*, 178–194.

(55) Inoue, S.; Browne, G.; Melino, G.; Cohen, G. M. Ordering of caspases in cells undergoing apoptosis by the intrinsic pathway. *Cell Death Differ.* **2009**, *16*, 1053–1061.

(56) Viola, G.; Cecconet, L.; Leszl, A.; Basso, G.; Brun, P.; Salvador, A.; Dall'Acqua, F.; Diana, P.; Barraja, P.; Cirrincione, G. Pyrrolotetrazinones deazaanalogues of Temozolomide induce apoptosis in Jurkat cell line: involvement of tubulin polymerization inhibition. *Cancer Chemother. Pharm.* **2009**, *64*, 1235–1251.

(57) Beswick, R. W.; Ambrose, H. E.; Wagner, S. D. Nocodazole, a microtubule depolymerising agent, induces apoptosis of chronic lymphocytic leukaemia cells associated with changes in Bcl-2 phosphorylation and expression. *Leukemia Res.* **2006**, *30*, 427–436.

(58) Vitale, I.; Antoccia, A.; Cenciarelli, C.; Crateri, P.; Meschini, S.; Arancia, G.; Pisano, C.; Tanzarella, C. Combretastatin CA-4 and combretastatin derivative induce mitotic catastrophe dependent on spindle checkpoint and caspase-3 activation in non-small cell lung cancer cells. *Apoptosis* **2007**, *12*, 155–166.

(59) Romagnoli, R.; Baraldi, P. G.; Cruz-Lopez, O.; Cara, C. L.; Carrion, M. D.; Brancale, A.; Hamel, E.; Chen, L.; Bortolozzi, R.; Basso, G.; Viola, G. Synthesis and antitumor ativity of 1,5-disubstituted 1,2,4-triazoles as cis-restricted combretastatin analogues. *J. Med. Chem.* **2010**, *53*, 4248–4258.

(60) Chen, Y.-C.; Lu, P.-H.; Pan, S. L.; Teng, C.-M.; Kuo, S.-C.; Lin, T.-P.; Ho, Y.-F.; Huang, Y.-C.; Guh, J.-H. Quinolone analogue inhibits tubulin polymerization and induces apoptosis via Cdk1-involved signaling pathways. *Biochem. Pharmacol.* **2007**, *74*, 10–19.

(61) McElligott, A. M.; Maginn, E. N.; Greene, L. M.; Siobhan McGuckin, S.; Hayat, A.; Browne, P. V.; Butini, S.; Campiani, G.; Catherwood, M. A.; Vandenberghe, E.; Williams, D. C.; Zisterer, D. M.; Mark Lawler, M. The novel tubulin-targeting agent pyrrolo-1,5-benzoxazepine-15 induces apoptosis in poor prognostic subgroups of chronic lymphocytic leukemia. *Cancer Res.* **2009**, *69*, 8366–8375.

(62) Hsieh, C.-C.; Kuo, Y.-H.; Kuo, C.-C.; Chen, L.-T.; Cheung, C.-H. A.; Chao, T.-Y.; Lin, C.-H.; Pan, W.-Y.; Chang, C.-Y.; Chien, S.-C.; Chen, T.-W.; Lung, C.-C.; Chang, J.-Y. Chamaecypanone C, a novel skeleton microtubule inhibitor, with anticancer activity by trigger caspase 8-Fas/FasL dependent apoptotic pathway in human cancer cells. *Biochem. Pharmacol.* **2010**, *79*, 1261–1271.

(63) Maginn, E. N.; Browne, P. V.; Hayden, P.; Vandenberghe, E.; MacDonagh, B.; Evans, P.; Goodyer, M.; Tewari, P.; Campiani, G.; Butini, S.; Williams, D. C.; Zisterer, D. M.; Lawler, M. P.; McElligott, A. M. PBOX-15, a novel microtubule targeting agent, induces apoptosis, upregulates death receptors, and potentiates TRAIL-mediated apoptosis in multiple myeloma cells. *Br. J. Cancer* **2011**, *104*, 281–289.

(64) Qi, Y.; Liao, F.; Zhao, C.; Lin, Y.; Zuo, M. Cytotoxicity, apoptosis induction, and mitotic arrest by a novel podophyllotoxin glucoside, 4DPG, in tumor cells. *Acta Pharmacol. Sin.* **2005**, *26*, 1000–1008.

(65) Yong, Y.; Shin, S. Y.; Lee, Y. H.; Lim, Y. Antitumor activity of deoxypodophyllotoxin isolated from *Anthriscus sylvestris*: Induction of G2/M cell cycle arrest and caspase-dependent apoptosis. *Bioorg. Med. Chem. Lett.* **2009**, *19*, 4367–4371.

(66) Shin, S. Y.; Yong, Y.; Kim, C. G.; Lee, Y. H.; Lim, Y. Deoxypodophyllotoxin induces G2/M cell cycle arrest and apoptosis in HeLa cells. *Cancer Lett.* **2010**, *287*, 231–239.

(67) Ko, S. C.; Johnson, V. L.; Chow, S. C. Functional characterization of Jurkat T cells rescued from CD95/Fas-induced apoptosis through the inhibition of caspases. *Biochem. Biophys. Res. Commun.* **2000**, *270*, 1009–1015.

(68) Sohn, D.; Schulze-Setoff, K.; Jänicke, R. U. Caspase-8 can be activated by interchain proteolysis without receptor-triggered dimerization during drug-induced apoptosis. *J. Biol. Chem.* **2005**, *280*, 5267–5273.

(69) Vermes, I.; Haanen, C.; Steffens-Nakken, H.; Reutelingsperger, C. A novel assay for apoptosis. Flow cytometric detection of phosphatidylserine expression on early apoptotic cells using fluorescein labelled Annexin V. *J. Immunol. Methods* **1995**, *184*, 39–51.

(70) Koopman, G.; Reutelingsperger, C. P.; Kuijten, G. A.; Keehnen, R. M.; Pals, S. T.; van Oers, M. H. Annexin V for flow cytometric detection of phosphatidylserine expression on B cells undergoing apoptosis. *Blood* **1994**, *84*, 1415–1420.

(71) Thurber, R. V.; Epel, D. Apoptosis in early development of the sea urchin, *Strongylocentrotus purpuratus*. *Dev. Biol.* **2007**, *303*, 336–346.

(72) Castedo, M.; Perfettini, J. L.; Roumier, T.; Andreau, K.; Medema, R.; Kroemer, G. Cell death by mitotic catastrophe: a molecular definition. *Oncogene* **2004**, *23*, 2825–2837.

(73) Titov, I. Y.; Sagamanova, I. K.; Gritsenko, R. T.; Karmanova, I. B.; Atamanenko, O. P.; Semenova, M. N.; Semenov, V. V. *Bioorg. Med. Chem. Lett.* **2011**, *21*, 1578–1581.